Geophysical Research Letters

RESEARCH LETTER
10.1029/2019GL083490

The Bunce Fault and Strain Partitioning in the Northern Lesser Antilles

M. Laurencin[1,2], B. Marcaillou[3], D. Graindorge[1], J.-F. Lebrun[4], F. Klingelhoefer[5], M. Boucard[4], M. Laigle[3], S. Lallemand[6], and L. Schenini[3]

[1]Laboratoire Géosciences Océan, UMR6538 CNRS-UBO-UBS, Université Bretagne Pays de Loire (UBL), Brest, Institut Universitaire Européen de la Mer, Plouzané, France, [2]Now at Earth Observatory of Singapore, Nanyang Technological University, Singapore, [3]Université Côte d'Azur, CNRS, Observatoire de la Côte d'Azur, IRD, Géoazur, Valbonne, France, [4]Géosciences Montpellier, UMR5243, Université des Antilles, CNRS, Université de Montpellier, Montpellier, France, [5]Géosciences Marines, Ifremer, ZI de la Pointe de Diable, Plouzané, France, [6]Géosciences Montpellier, CNRS, Université de Montpellier, Université des Antilles, Montpellier, France

Abstract Strain partitioning related to oblique plate convergence has long been debated in Northern Lesser Antilles. Geophysical data acquired during the ANTITHESIS cruises highlight that the sinistral strike-slip Bunce Fault develops along the vertical, long, and linear discontinuity between the sedimentary wedge and a more rigid backstop. The narrowness of the 20- to 30-km-wide accretionary wedge and its continuity over ~850 km is remarkable. The Bunce Fault extends as far south as 18.5°N where it anastomoses within the accretionary prism where the sharp increase in convergence obliquity possibly acts as a mechanical threshold. Surface traces related to subducting seamounts suggest that 80% of the lateral component of the convergent motion is taken up by internal deformation within the accretionary prism and by the Bunce Fault. The absence of crustal-scale, long-term tectonic system south of the Anegada Passage casts doubt upon the degree of strain partitioning in the Northern Lesser Antilles.

Plain Language Summary Lithospheric plates are frequently bounded by subduction zones where oceanic plates underthrust overriding plates. In most cases, this convergence is oblique to the margin, its resulting tectonic deformation is generally due to margin-normal and margin-parallel components of the plate convergence vector. At the Northern Lesser Antilles, the North American Plate subducts beneath the Caribbean Plate with oblique convergence increasing from Guadeloupe to Virgin Islands. This study aims to analyze and resolve the tectonic deformation along this margin. We acquired marine geophysical data during ANTITHESIS cruises (2014–2016) to image the seafloor and the crustal structure. We place a particular emphasis on the strike-slip Bunce Fault, which extends over ~850 km, including a newly discovered 350-km segment, 20–30 km landward from the trench. Although long strike-slip faults have already been observed at oblique subduction zones, the proximity of the Bunce Fault to the trench is unprecedented. We conclude that the mechanical discontinuity between the sedimentary wedge and a more rigid backstop and the sharp increase in obliquity is likely to control the location of the trench-parallel, strike-slip deformation north of the Anegada Passage when strain partitioning to the south may be small or taken up in more diffuse pattern.

Key Points:
- ANTITHESIS cruises highlight the SE extent of the Bunce Fault where it anastomoses in the prism at the change of obliquity of convergence
- The sinistral strike-slip Bunce Fault develops along a rheological discontinuity at the prism backstop at 30 km from the trench
- A synthesize of structures resulting from strain partitioning observed in the Greater and Northern Lesser Antilles is proposed

Supporting Information:
- Supporting Information S1

Correspondence to:
M. Laurencin,
muriel.laurencin@univ-brest.fr

Citation:
Laurencin, M., Marcaillou, B., Graindorge, D., Lebrun, J.-F., Klingelhoefer, F., Boucard, M., et al. (2019). The Bunce Fault and strain partitioning in the Northern Lesser Antilles. *Geophysical Research Letters*, *46*, 9573–9582. https://doi.org/10.1029/2019GL083490

Received 26 APR 2019
Accepted 8 AUG 2019
Accepted article online 16 AUG 2019
Published online 30 AUG 2019

1. Introduction

Convergence obliquity greater than 27° occurs in more than ~50% of subduction zones worldwide (Heuret, 2005) as, for instance, in Sumatra (McCaffrey, 1991), Taiwan (Lallemand et al., 1999), or the Philippines (Quebral et al., 1996). High obliquity and strong basal friction favor strain partitioning into trench-normal and trench-parallel components (Chemenda et al., 2000; Fitch, 1972). The trench-normal component is taken up by fold-thrusts belts, the trench-parallel component, by strike-slip systems (Mann, 2007). The systems in the arc and forearc are frequently long (>600 km), penetrating at crustal or lithospheric scale, bounding landward laterally moving slivers and located away from the trench (Chemenda et al., 2000; Philippon & Corti, 2016). The Great Sumatran Fault (McCaffrey, 1991), the Median Tectonic Line in Nankai (e.g., Ikeda et al., 2009), and the Philippines fault (Quebral et al., 1996) are major examples of such strike-slip systems. In contrast, only few examples of strike-slip faults located close to the trench are documented. They develop along major structural/rheological discontinuity as at the accretionary wedge backstop (Chemenda et al., 2000; Lallemand et al., 1999), branch downward onto the subduction interface, and separate a laterally

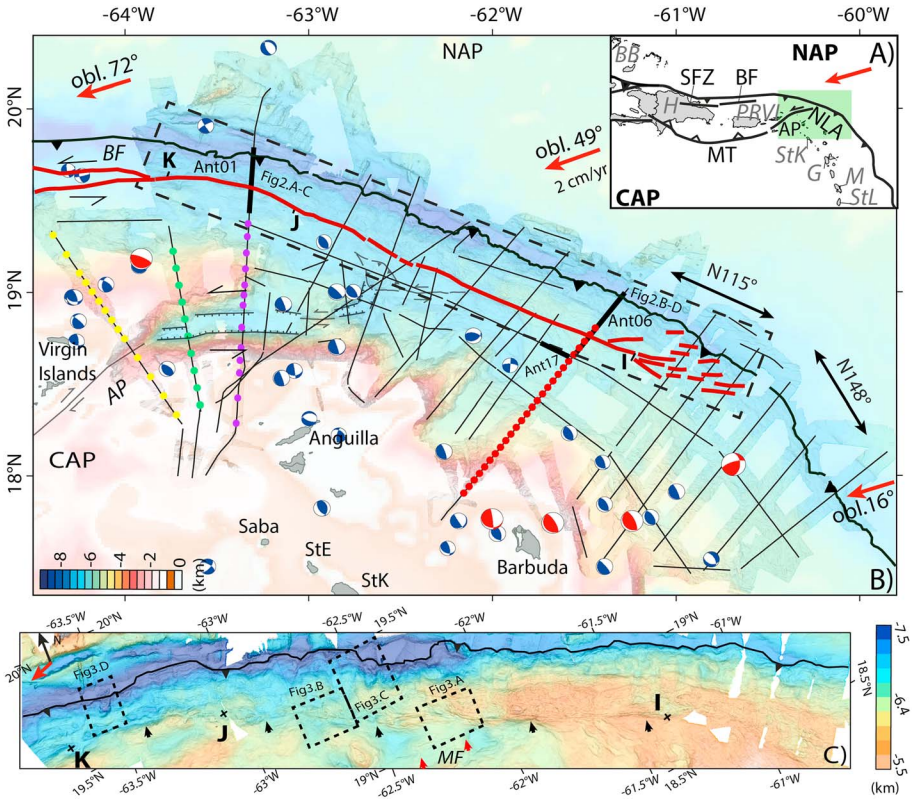

Figure 1. (a) Geodynamic setting of the northeastern Caribbean Plate boundary. (b) Bathymetric map showing location of multichannel seismic data (black lines) and wide-angle seismic data (colored circles at ocean-bottom seismometer location) recorded during cruises ANTITHESIS 1 and 3. Structures at the Anegada Passage (thin gray lines) are from Laurencin et al. (2017) and the Bunce Fault (thick red line) from this study and ten Brink et al. (2004). Close-up in Figure 2 are located along thick black lines. Focal mechanisms for earthquakes with a $Mw > 4.5$ and 5.5 are, respectively, in blue and red. (c) Bathymetric close-up corresponding to the dashed frame in (b) and showing the Bunce Fault (black arrows) and the Malliwana Fault (small red arrows). Dashed boxes encompass 2-D close-up in Figure 3. Red arrows stand for convergence vector between North American (NAP) and Caribbean (CAP) Plates (DeMets et al., 2000). AP: Anegada Passage, BB: Bahamas Bank, G: Guadeloupe, H: Hispaniola, M: Martinique, MT: Muertos Trough, NLA: Northern Lesser Antilles, PRVI: Puerto Rico Virgin Islands, SFZ: Septentrional Fault Zone, StE: St Eustatius, StK: Saint Kitts, StL: St Lucia.

moving and deforming sedimentary wedge sliver. Various studies have addressed the question of tectonic deformation related to strain partitioning along the Antilles subduction zones: from Hispaniola to Puerto Rico where it has been clearly identified (Mann et al., 2005; ten Brink et al., 2004) and from the Virgin Islands to Guadeloupe where it is poorly imaged and more hotly debated (Bouysse, 1988; Bouysse & Westercamp, 1990; Calais et al., 2016; Feuillet et al., 2002; Feuillet et al., 2011; López et al., 2006; Manaker et al., 2008; Symithe et al., 2015).

During ANTITHESIS 1, "ANTIlles THErmicité and SISmicité," (Marcaillou & Klingelhoefer, 2013) and ANTITHESIS 3 cruises (Marcaillou & Klingelhoefer, 2016), we acquired multibeam bathymetric data and the first deep seismic images in the Northern Lesser Antilles (NLA) and the eastern Puerto Rico Virgin Islands (PRVI) margin segments (Figure 1). This data set highlights a 350-km-long, trench-parallel, prominent strike-slip fault (Figure 1) located 30 km from the trench. This newly discovered fault segment extends southward from the Bunce Fault described further west by ten Brink et al. (2004). This study (1) provides evidence for its long-term left-lateral deformation, (2) shows its southeastern extremity and the relation with the plate convergence obliquity, and (3) highlights the geological and structural context of the fault at this location. These observations show the influence of increasing plate convergence obliquity on the development of subduction-linked strike-slip faults. This allows us to propose a large-scale model for active partitioning systems in the NLA.

2. Geological and Tectonic Background

At the northeastern limit of the Caribbean Plate, along the Lesser Antilles subduction zone, the North American Plate subducts beneath the convex NLA and PRVI margin segments with a plate convergence rate of ~20 mm/year in a ~N254° direction (DeMets et al., 2000). The plate convergence obliquity, relative to trench-normal direction, progressively increases along the trench as it curves northwestward (Figure 1). Obliquity ranges from ~0° to 75°, from the latitude of Guadeloupe to Puerto Rico Trench, respectively. Farther west, the subduction turns into a sinistral strike-slip plate boundary to the west of Hispaniola (Figure 1; e.g., Sykes et al., 1982; Mann & Burke, 1984). Various studies have addressed the question of tectonic deformation related to strain partitioning along NLA and PRVI margins. Mann et al. (2005) summarize these tectonic studies at the PRVI microplate between southward underthrusting along the Puerto Rico Trench and northward underthrusting along the Muertos Trough. The collision of the Bahamas Bank with the northern Caribbean margin since the late Paleogene (e.g., Pindell & Kennan, 2009) led to inception of the North Caribbean strike-slip Plate boundary and motion partitioning along the NLA-PRVI margins as the trench curvature initiated (Legendre et al., 2018). During the Miocene, the Anegada Passage possibly accommodated transtensive relative motion between Caribbean and PRVI block in response to this collision (e.g., Jany et al., 1990; Mann et al., 2005). Later on, this transtensive extension was stopped and the structures are recently reactivated by a left-laterally partitioning system (Figure 1; Laurencin et al., 2017) as also substantiated by GPS data interpretation (Jansma & Mattioli, 2005). To the north of the Anegada Passage, the strike-slip Bowin Fault extends eastward the Septentrional Fault of Hispaniola and connects with the left-lateral strike-slip Bunce Fault (Grindlay et al., 2005). The Bunce Fault extends over 530 km between 68.5°W and 62.3°W located at only 10–20 km landward from the Puerto Rico Trench (ten Brink et al., 2004). To the south of the Anegada Passage, Feuillet et al. (2002; 2011) interpreted arc-perpendicular grabens in the forearc domain and a set of en echelon short transtensional right-stepping faults along the volcanic arc from Martinique to Saint Kitts as the expression of strain partitioning. López et al. (2006) proposed that discrepancies between predicted directions of North America and Caribbean Plates convergence and slip vectors of thrust fault earthquakes suggest that the NLA forearc moves independently as a block distinct from both major plates. These observations led them to propose that a ~800 × 300 km northward drifting arc-forearc sliver extends from southern Martinique Island up to the Puerto Rico Trench. Tectonic interpretations based on GPS networks located onshore NLA Islands, only, result in diverging conclusions. Based on kinematic models of microblocks derived from GPS data, without considering the Bunce Fault, the PRVI and NLA margin segments possibly undergo oblique subduction either without any strain partitioning (Calais et al., 2016; Manaker et al., 2008; Symithe et al., 2015) or with left-lateral strike-slip relative motion (Jansma & Mattioli, 2005).

3. Data and Processing

Coincident multichannel seismic (MCS) lines Ant01 and Ant06 and wide-angle seismic data AN1 and AN6 (Figure 1) were acquired using a 3.75-km-long 300-channel-streamer, 39 ocean-bottom seismometers and 7699-in.^{3} tuned air gun array. MCS quality-control and processing were performed with SolidQC® and GEOVATION®, respectively, as detailed in Laurencin et al. (2017). AN1 and AN6 *P* wave velocity (*Vp*) models were built using a forward modeling approach (Zelt & Smith, 1992; Figure 2). Methods, processing, velocity modeling, and resolution tests are described in Laurencin et al. (2018). We also processed multichannel bathymetric data acquired during these cruises and calculated digital elevation models at 100- and 75-m grid spacing using the CARAIBES® software. This digital elevation model was further analyzed using free software Qgis. Uninterpreted MCS lines and bathymetric map are provided in the supporting information.

4. Observations: The Bunce Fault

A prominent bathymetric lineament parallel to the deformation front is located 20 to 30 km arcward of the trench, offshore from Barbuda to the Virgin Islands (Figure 1c). Trench-parallel, obliquely oriented bathymetry reveals that the N112° trending lineament is mostly rectilinear with local discontinuities from I to J (Figure 1c). To the NW, from J to K, the lineament veers slightly and connects westward to the N90° striking Bunce Fault observed offshore Virgin Islands and Puerto Rico (ten Brink et al., 2004; Figure 1c). At depth, in MCS lines, this lineament corresponds to steep planes that converge downward likely soling out onto the

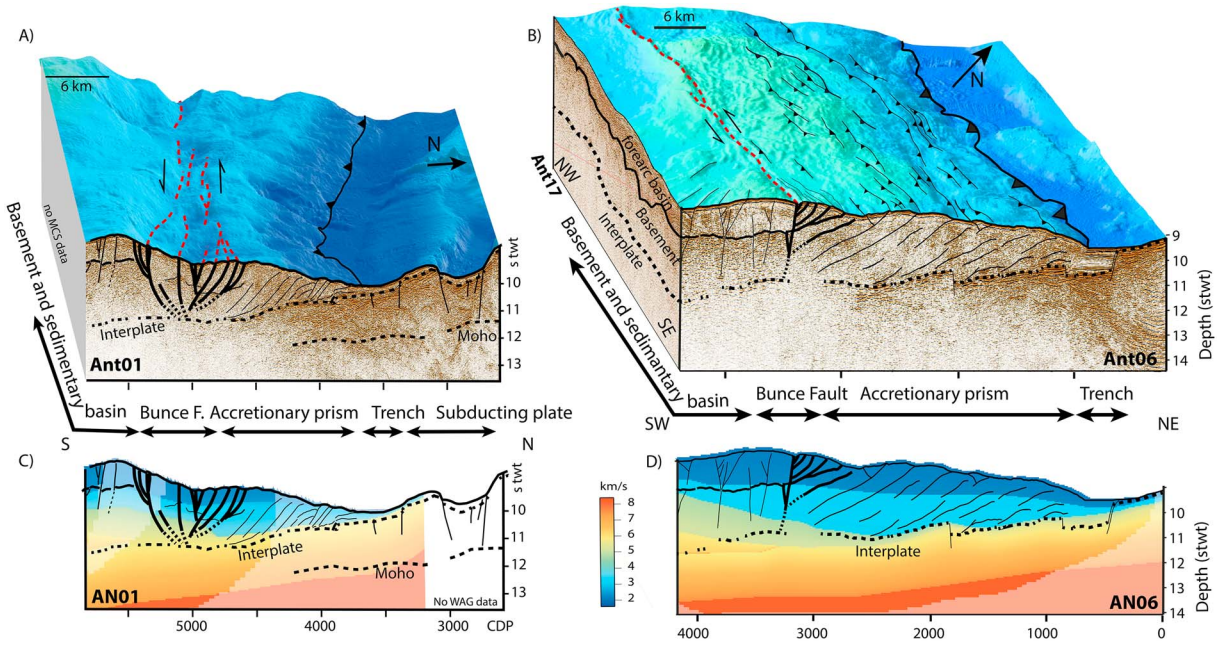

Figure 2. Three-dimensional seismic bathymetry view for lines Ant01 (a) and Ant06/Ant17 (b) with corresponding *Vp* model, AN01 (c) and AN06 (d), derived from wide-angle data converted in second two-way travel time. See thick black lines in Figure 1 for location. Pale colors in (c) and (d) extend velocity models where unconstrained by seismic data.

plate interface and outcropping at the seafloor, for instance at CDP 4600-5300 in Line Ant01 (Figure 2a) and at CDP 2700-3200 in Line Ant06 (Figure 2b; see also MCS lines in the supporting information). These steep planes vertically offset the seafloor and the internal reflectors define negative (Figure 2a) or positive (Figure 2b) flower structures. In map view, sigmoidal left/right-stepping fault segments connect through bathymetric depressions/highs (Figures 2, 3a, and 3b) indicating transtensive/transpressive relays, which are typical of sinistral strike-slip deformation. The length, linearity, steepness, and flower shape of the fault are consistent with a strike-slip system at a mature stage of its development (Martinez et al., 2002), showing that the Bunce Fault extends south as far as 18.65°N.

WAS-derived seismic velocities and MCS lines highlight the nature of margin structures along which the Bunce Fault developed at the PRVI (Line Ant01) and NLA (Line Ant06) margin segments. These data reveal contrasted seismic facies and velocities across the Bunce Fault. *Vp* changes rapidly across the fault zone, with a significant arcward increase of the vertical gradient. From the deformation front to the fault, velocity varies vertically from 2.5 km/s beneath the seafloor to 3 km/s above the interplate contact at 10-km depth (Figures 2c and 2d). In contrast, at similar depths to the southwest of the fault, velocity varies vertically from 2.5 to 5.5–6 km/s. Thus, at crustal depth, velocity increases landward from 3 to 5.5–6 km/s across the Bunce Fault (Figures 2c and 2d). In addition, this lateral velocity contrast coincides with a drastic change in the seismic facies in MCS lines. On the trenchward side of the fault, MCS data show series of landward dipping reflectors typical of in-sequence thrusts in imbricated fold and thrust belt of an accretionary prism. The thrust faults outcrop at the seafloor, shift upward local reflector packages, and sole out at depth onto the interplate contact (Figures 2a and 2b). These dipping reflectors are associated with trench-parallel bathymetric lineaments that bound folded ridges and piggyback basins. In contrast, on the landward side of the fault, the smoother seafloor tops a ~1-s two-way travel time thick upper seismic unit of irregularly bedded reflectors. This unit unconformably rests upon high-amplitude low-frequency reflections at the roof of a 2.5-s two-way travel time thick chaotic, poorly reflective lower seismic unit. These units likely correspond to the forearc sedimentary basin and the high-velocity margin current basement, respectively. Thus, wide-angle *Vp* and seismic facies indicate that the sinistral strike-slip Bunce Fault separates the 20- to 30-km-wide accretionary prism from a crustal margin backstop.

To the east of I (I letter on Figure 1), the morphologic expression of the Bunce Fault changes from a narrow deformation zone to a 60-km-long, 30-km-wide anastomosing system that vanishes southward (Figures 1

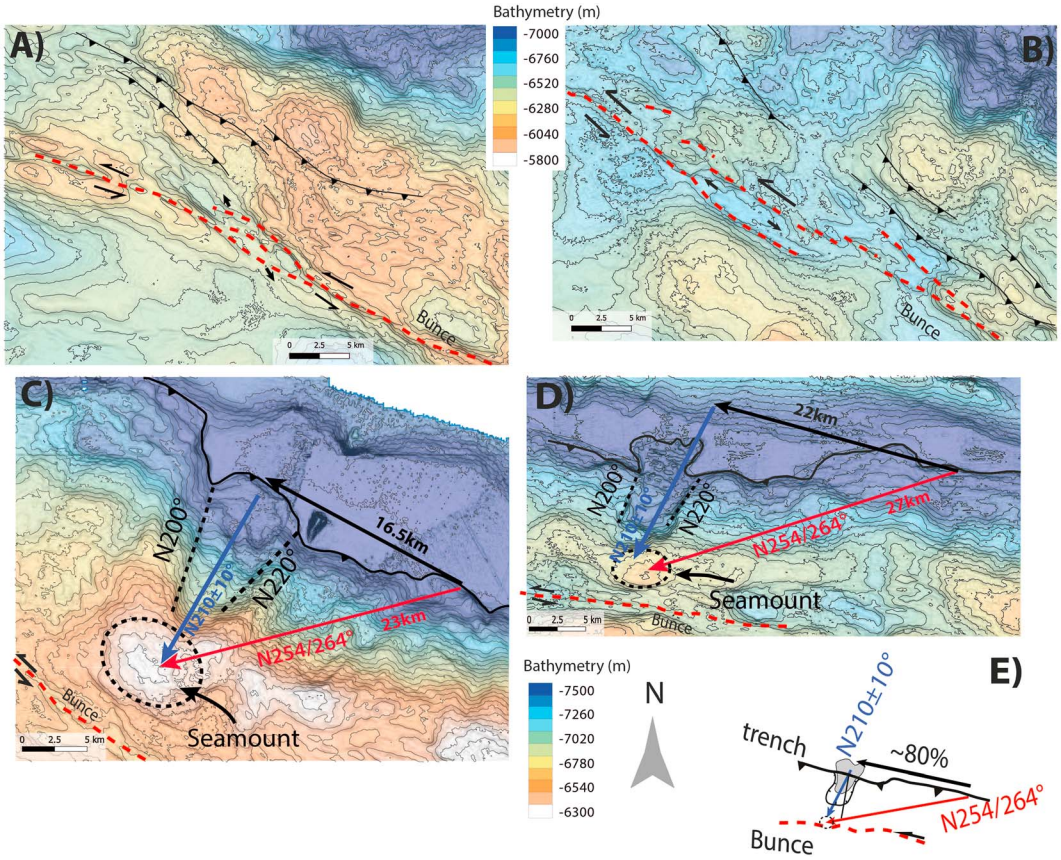

Figure 3. Two-dimensional bathymetric view for (a and b) narrow elongate pull-apart basins at left stepping en echelon relays along the Bunce Fault and (c and d) scars in the margin wedge and mass-wasting in the trench related to seamounts subduction. Gray thin lines show 50-m contours. Red and blue arrows (e) indicate relative plate motion (N254–264°) and mass wasting direction trending parallel to the trailing edge of the scars (N210 ± 10°). Discrepancy between those directions highlights northwestward motion of the margin wedge (explanations in the text) of ~80% of the convergence rate. See black frames in Figure 1c for location of 2-D views.

and 4). To the north of this anastomosing system, straight N140° trending bathymetric slope lineaments show the surface trace of outcropping thrust faults in the prism (Figure 4). In contrast, within the anastomosing system, the thrusts surface traces are left-laterally shifted, in sigmoidal shape (see white ellipses in Figure 4) along N100-110° directed short bathymetric lineaments that converge toward the Bunce Fault in I. This system departs from the trend of the margin backstop whose orientation changes from N110° to N130°, as identified on MCS lines (red dots in Figure 4). Further south, Line Ant45, for instance, confirms the absence of flower structure located at the accretionary prism backstop at this latitude (supporting information). In contrast, at CDP 2000–2200 and 2800–3000, this line shows small and shallow flower structures that sole out downward onto thrust fault in the prism and correspond with N110° trending bathymetric lineaments (Figure 4). The MCS and bathymetric data thus define anastomosing strike-slip fault segments connecting with the accretionary wedge thrusts and folds belt that are therefore likely to accommodate oblique slip at the eastern ending of the Bunce system. This termination is located near an abrupt change in the trench orientation, which results in a southward decrease in convergence obliquity, from 49° to 16° (Figure 1). Thus, conversely, the northward sharp increase in convergence obliquity possibly acts as a mechanical threshold favoring the onset of strike-slip deformation. This deformation generates a diffuse zone of oblique slip along short fault segments within the accretionary prism that merge northwestward within short distances into a long rectilinear mature strike-slip fault located at the backstop of the accretionary wedge.

In oblique convergent margins, where seamounts enter the trench and interact with the margin wedge, the azimuth of deformation traces left behind them, compared to plate convergence direction, allows estimating

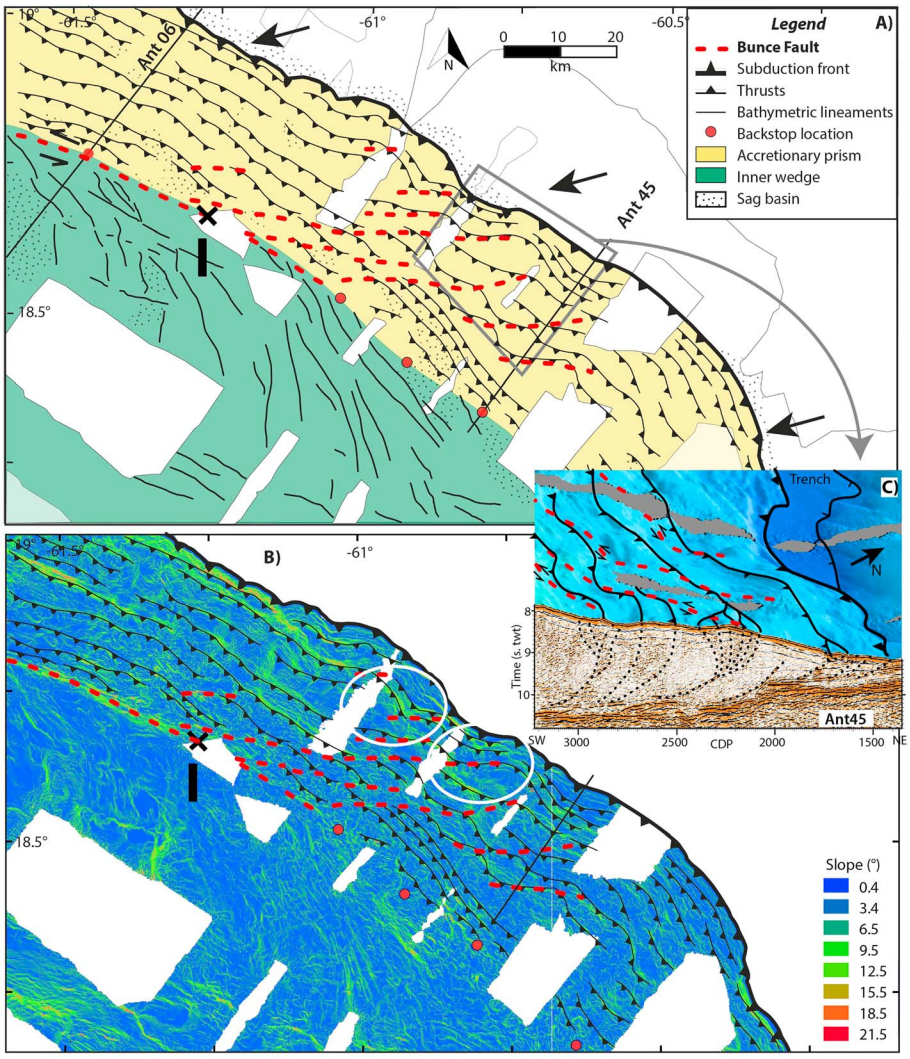

Figure 4. (a) The morphostructural and (b) the slope maps at the southern end of the Bunce Fault (see location of I in Figure 1) showing the anastomosing system. White ellipses show thrust surface expressions shifted by left-lateral motion by the Bunce Fault lineament terminus. (c) 3-D seismic-bathymetry view for Line Ant45 in the accretionary prism.

the lateral motion of the wedge (e.g., Dominguez et al., 1998; Ranero & von Huene, 2000). When this azimuth is subparallel to plate convergence vector, the wedge lateral motion is insignificant. In any case, this azimuth provides a rough estimate for this lateral motion. The North American Plate is covered with seamounts (Laurencin, 2017) that approach the trench with N254–264° direction (DeMets et al., 2000; Jansma & Mattioli, 2005). In contrast, the surface deformation traces for subducting seamounts are directed N210 ± 10° (Figures 3c and 3d). Given the curved shape of these traces, a 20° uncertainty is assumed. This ~50 ± 10° angle to the northwest of the plate convergence vector with respect to the seamount-related deformation traces indicates a northwestward displacement of the margin wedge.

5. Discussion: Strain Partitioning in the NLA

5.1. Left-Lateral Deformation

This ~50 ± 10° angle to the northwest of the plate convergence vector with respect to the seamount-related deformation traces indicates a northwestward motion of the margin wedge of 80 ± 10% of the plate convergence. This rough estimate suggests a 1.6 ± 0.2-cm/year lateral motion of the accretionary prism. This motion is taken up partly by internal deformation within the accretionary prism and partly by sinistral

strike-slip motion along the Bunce Fault. In absence of additional constraints from in situ GPS data, seismological monitoring and geological sampling, an estimate for slip rate along the Bunce Fault is speculative. The ages of the Bunce Fault and of the innermost accretionary units are unknown. Moreover, the bathymetric map does not show any lineament across the backstop and the sedimentary prism, whose lateral shift could provide constraints about this slip rate. As a result, seamount-related deformation traces provide a rough estimate for maximum slip rate along the Bunce Fault. Considering the hypothesis of a laterally moving nondeformable rigid sliver, the slip rate along the Bunce Fault would be 1.6 ± 0.2 cm/year.

5.2. Convergence Obliquity Variation and Anastomosing Strike-Slip Fault

Analogue modeling (Martinez et al., 2002) and in situ observations (Jarrard, 1986; McCaffrey, 1992) suggest that low subduction obliquity (~15°) is sufficient to trigger strain partitioning. These results are consistent with the Central Lesser Antilles and NLA where convergence obliquity increases progressively northward from ~0° to 16° from Guadeloupe to Antigua latitudes then changes to 49° north of the 18.5°N kink in the deformation front (Figure 1). The strike-slip Bunce system easternmost termination is currently located near this increase in convergence obliquity (Figure 1). In contrast, to the south of 18.5°N kink, where the obliquity is low, bathymetric and seismic data acquired during ANTITHESIS (this study and Laurencin, 2017) do not image localized strike-slip deformation in the accretionary wedge or at the backstop. We conclude that deformable accreted sediments, low basal friction and arcward dipping, discontinuous, deformed backstop (Laigle et al., 2013) tend to impede strike-slip deformation localization at low to intermediate plate convergence obliquity. In contrast, the sharp increase in this obliquity at 18.5°N possibly acts as a mechanical threshold favoring strain partitioning that focusses strike-slip deformation at trench-parallel, vertical and continuous rheological discontinuity of the current wedge backstop.

5.3. Bunce Fault Proximity to the Trench

The 850-km-long Bunce Fault is located intriguingly close to the trench in the NLA and offshore Puerto Rico, compared to more inland strike-slip faults in Hispaniola. Ten Brink and Lin (2004) proposed that this variation in the strike-slip fault distance to the trench, from Puerto Rico to Hispaniola, is related to different distributions of Coulomb stress in the forearc region, as a result of the change from the nearly trench-parallel slip on the Puerto Rico subduction interface to the more perpendicular subduction slip beneath Hispaniola (ten Brink & Lin, 2004). This explanation may not be suitable to the southeast of Puerto Rico, where slip obliquity for thrust earthquakes decreases down to ~30° and to a few degrees south of Barbuda (López et al., 2006; Figure 1). This obliquity is close to that at Hispaniola, but the Bunce Fault remains close to the trench over an additional 350-km-long distance. The data presented here support an alternate explanation for this proximity to the trench. The Bunce Fault branches out at the backstop (i.e., at the transition between the accretionary prism and the lithified forearc basin sediment and crustal basement rocks), which is a long and continuous inherited weakness zone in the margin. Previous studies pointed out the control of this weakness in localizing the strike-slip motion at backstop (e.g., Chemenda et al., 2000). However, strike-slip faults associated to wedge weakness at a short distance from the deformation front are usually local as in Nankai (Tsuji et al., 2014) or Southern Ryukyu (Lallemand et al., 1999).

The Bunce Fault forms a structural boundary separating the very narrow, sediment-starved trench, or deformation front. A larger sediment supply would have probably resulted in a wider prism and a greater distance between the trench and the fault. Thus, in the context of long-term margin erosion, we cannot rule out the scenario of a strike-slip system that initiated at greater distance from the trench, at the rear of an initially larger and progressively eroded accretionary domain. However, the Bunce Fault proximity to the trench is likely to be primarily controlled by the major mechanical weakness at the toe of the prism backstop which has the exceptional character of being straight and both vertically and laterally sharp over long distances.

5.4. Overview of Strike-Slip Structures in the Margin

In the following, we present an overview of the published structural observations for major lithospheric tectonic deformation related to the strain partitioning at NLA margin. The inherited E-W trending forearc segment of the Anegada Passage has been reactivated in a sinistral strike-slip system that connects eastward to the Bunce Fault (Figures 1 and 5; Laurencin et al., 2017). GPS data indicate that relative block motions are taken up along the Anegada Passage, with low velocity of 1.2 mm/year, (Jansma & Mattioli, 2005) up to 1.8 mm/year (Calais et al., 2016), close to the uncertainty estimate.

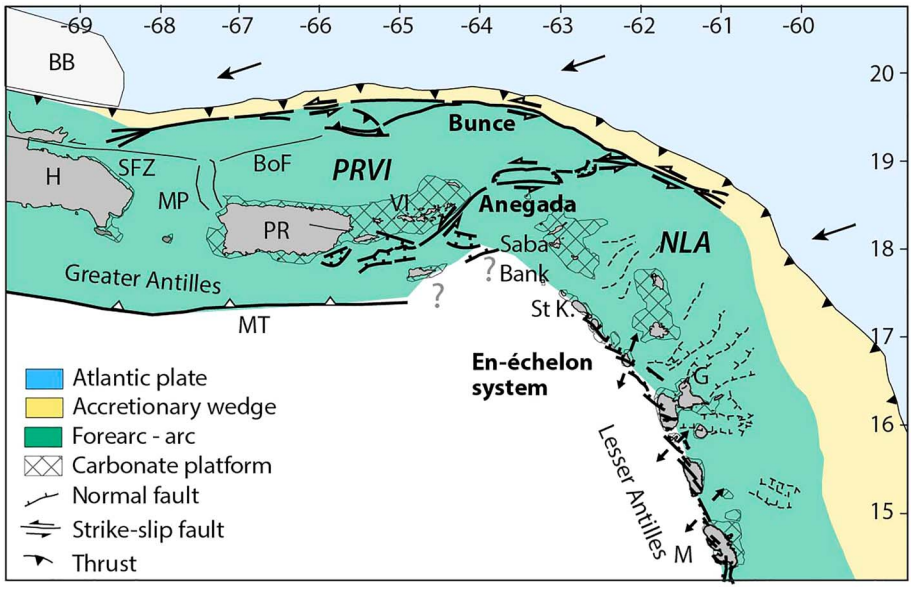

Figure 5. Summary of observed and imaged tectonic structures interpreted as related to strain partitioning at the PRVI and NLA margin segments. BB: Bahamas Bank, G: Guadeloupe, H: Hispaniola, M: Martinique, MT: Muertos Thrust, MP: Mona Passage, NLA: Northern Lesser Antilles, PR: Puerto Rico, PRVI: Puerto Rico Virgin Islands block, St K: Saint Kitts, VI: Virgin Islands. BoF: Bowin Fault and SFZ: Septentrional Fault Zone after Grindlay et al. (2005). The location of the accretionary wedge backstop in the Central Antilles is from Laigle et al. (2013).

To the southeast, right-stepping short en echelon faults system (Figure 5) are discontinuously distributed along the arc from Martinique to Saint Kitts islands (Feuillet et al., 2002, 2011) and do not extend farther northwest through the Saba's Bank (Lebrun et al., 2017) and the Anegada Passage (Laurencin et al., 2017). This tectonic system differs from hundreds-of-kilometer-long, crustal-scale, continuous strike-slip systems observed along forearcs and arcs undergoing strain partitioning: the Great Sumatran Fault (McCaffrey, 1991), the Median Tectonic Line in Nankai (e.g., Ikeda et al., 2009), and the Philippine fault (Quebral et al., 1996).

In contrast with the Greater Antilles margin, these observations question about the total amount of relative motion along tectonic structures related to strain partitioning to the south of the Anegada Passage. Analogue (e.g., Leever et al., 2011) and numerical (e.g., Chemenda et al., 2016) modeling show that the early stages of strike-slip deformation consist in oblique short en echelon normal to transtensive faults, which progressively rotate to a direction more closely parallel to the shear strain and coalesce in a long and continuous strike-slip system. The en echelon fault system along the Lesser Antilles arc has not yet coalesced into a mature strike-slip fault suggesting that, on a longer time scale, the total amount of slip accommodated by this system is low.

In addition, identified earthquakes associated to this system, south of Guadeloupe show normal-faulting mechanisms. Only two strike-slip events occurred along a fault segment north of Montserrat (González et al., 2017, and references therein). Moreover, although GPS networks are located onshore arc islands only, geodetic modeling does not confirm systematic differential motion between forearc and back-arc domains (Symithe et al., 2015). A wider GPS location in an E-W direction would provide more solid constraints on this point. As a result, interpretations concerning the amount of strain partitioning in the forearc diverge. Calais et al. (2016) interpret oblique slip with no partitioning at the scale of PRVI and NLA block, while Turner et al. (2008) propose a laterally moving and internally deforming Northern Lesser Antilles Arc/Forearc sliver.

The straight long 850-km-long Bunce Fault limits a narrow and thin sedimentary prism. Thus, in the absence of a major long-term tectonic system at crustal scale, plate motion at NLA could be mostly unpartitioned south of the Anegada Passage. Alternately, strain partitioning could be taken up along pervasive short systems in a more diffuse pattern at margin scale, possibly owing to low interplate friction or lesser obliquity.

Acknowledgments

We thank the Captain and Crew of RVs L'Atalante and Pourquoi Pas?, the Genavir Technicians and Engineers for processing of bathymetric data and for acquisition of seismic, and the Scientific Crew for preprocessing performed onboard. We acknowledge financial support from Region Bretagne for the PhD fellowship of M. Laurencin. We thank Labex MER, INSU, and Antilles University for contributing to the costs of the cruises. We thank native English-speaking Dr. Marc-André Gutscher for correcting the English language of the manuscript. Most of figures were drafted using GMT and Qgis software. MCS data were processed with Geovation software of CGG. All data of the ANTITHESIS cruises are available upon request at the SISMER data archive (https://doi.org/10.18142/242).

References

Bouysse, P. (1988). Opening of the Grenada back-arc Basin and evolution of the Caribbean plate during the Mesozoic and early Paleogene. *Tectonophysics*, *149*(1-2), 121–143. https://doi.org/10.1016/0040-1951(88)90122-9

Bouysse, P., & Westercamp, D. (1990). Subduction of Atlantic aseismic ridges and Late Cenozoic evolution of the Lesser Antilles island arc. *Tectonophysics*, *175*(4), 349–380. https://doi.org/10.1016/0040-1951(90)90180-G

Calais, E., Symithe, S. J., Mercier De Lepinay, B., & Prépetit, C. (2016). Plate boundary segmentation in the northeastern Caribbean from geodetic measurements and Neogene geological observations. *Comptes Rendus Geosciences*, *348*(1), 42–51. https://doi.org/10.1016/j.crte.2015.10.007

Chemenda, A., Cavalié, O., Vergnolle, M., Bouisson, S., & Delouis, B. (2016). Numerical model of formation of a 3-D strike-slip fault system. *Comptes Rendus Geoscience*, *348*(1), 61–69. https://doi.org/10.1016/j.crte.2015.09.008

Chemenda, A., Lallemand, S., & Bokun, A. (2000). Strain partitioning and interplate friction in oblique subduction zones: Constraints provided by experimental modeling. *Journal of Geophysical Research*, *105*(B3), 5567–5581. https://doi.org/10.1029/1999JB900332

DeMets, C., Jansma, P., Mattioli, G., Dixon, T. H., Farina, F., Bilham, R., et al. (2000). GPS geodetic constraints on Caribbean-North America plate motion. *Geophysical Research Letters*, *27*(3), 437–440. https://doi.org/10.1029/1999GL005436

Dominguez, S., Lallemand, S. E., Malavieille, J., & von Huene, R. (1998). Upper plate deformation associated with seamount subduction. *Tectonophysics*, *293*(3-4), 207–224. https://doi.org/10.1016/S0040-1951(98)00086-9

Feuillet, N., Beauducel, F., & Tapponnier, P. (2011). Tectonic context of moderate to large historical earthquakes in the Lesser Antilles and mechanical coupling with volcanoes. *Journal of Geophysical Research*, *116*, B10308. https://doi.org/10.1029/2011JB008443

Feuillet, N., Manighetti, I., Tapponnier, P., & Jacques, E. (2002). Arc parallel extension and localization of volcanic complexes in Guadeloupe, Lesser Antilles. *Journal of Geophysical Research*, *107*(B12), 2331. https://doi.org/10.1029/2001JB000308

Fitch, T. J. (1972). Plate convergence, transcurrent faults, and internal deformation adjacent to Southeast Asia and the western Pacific. *Journal of Geophysical Research*, *77*(23), 4432–4460. https://doi.org/10.1029/JB077i023p04432

González, O.-L., Clouard, V., & Zahradnik, J. (2017). Moment tensor solutions along the central Lesser Antilles using regional broadband stations. *Tectonophysics*, *717*, 214–225. https://doi.org/10.1016/j.tecto.2017.06.024

Grindlay, N. R., Mann, P., Dolan, J. F., and Van Gestel, J. P. 2005. Neotectonics and subsidence of the northern Puerto Rico-Virgin Islands margin in response to the oblique subduction of high-standing ridges. Edited by Paul Mann. Geological Society of America Special Papers 385: 31–60.-Leg1 Cruise

Heuret, A. 2005. Dynamique des zones de subduction: Etude statistique globale et approche analogique. Montpellier II.

Ikeda, M., Toda, S., Kobayashi, S., Ohno, Y., & Nishizaka, N. (2009). Tectonic model and fault segmentation of the Median Tectonic Line active fault system on Shikoku, Japan. *Tectonics*, *28*, TC5006. https://doi.org/10.1029/2008TC002349

Jansma, P. E., and Mattioli, G.S. 2005. GPS results from Puerto Rico and the Virgin Islands: Constraints on tectonic setting and rates of active faulting. In *Mann P*., 13–30. Active tectonics and seismic hazards of Puerto Rico, the Virgin Islands, and offshore areas: Geological Society of America Special Paper 385. doi:10.1130/0-8137-2385-X.13.

Jany, I., Scanlon, K. M., & Mauffret, A. (1990). Geological interpretation of combined Seabeam, Gloria and seismic data from Anegada Passage (Virgin Islands, north Caribbean). *Marine Geophysical Researches*, *12*(3), 173–196. https://doi.org/10.1007/BF02266712

Jarrard, R. D. (1986). Terrane motion by strike-slip faulting of forearc slivers. *Geology*, *14*(9), 780. https://doi.org/10.1130/0091-7613(1986)14<780:TMBSFO>2.0.CO;2

Laigle, M., Becel, A., de Voogd, B., Sachpazi, M., Bayrakci, G., Lebrun, J. F., & Evain, M. (2013). Along-arc segmentation and interaction of subducting ridges with the Lesser Antilles Subduction forearc crust revealed by MCS imaging. *Tectonophysics*, *603*, 32–54. https://doi.org/10.1016/j.tecto.2013.05.028

Lallemand, S., Liu, C.-S., Dominguez, S., Schnürle, P., & Malavieille, J. (1999). Trench-parallel stretching and folding of forearc basins and lateral migration of the accretionary wedge in the southern Ryukyus: A case of strain partition caused by oblique convergence. *Tectonics*, *18*(2), 231–247. https://doi.org/10.1029/1998TC900011

Laurencin, M. 2017. Etude de la géométrie, de la nature et des déformations de la zone de subduction des Petites Antilles du Nord. Université de Bretagne Occidentale - Université Bretagne Loire.

Laurencin, M., Graindorge, D., Klingelhoefer, F., Marcaillou, B., & Evain, M. (2018). Influence of increasing convergence obliquity and shallow slab geometry onto tectonic deformation and seismogenic behavior along the Northern Lesser Antilles zone. *Earth and Planetary Science Letters*, *492*, 59–72. https://doi.org/10.1016/j.epsl.2018.03.048

Laurencin, M., Marcaillou, B., Graindorge, D., Klingelhoefer, F., Lallemand, S., Laigle, M., & Lebrun, J. F. (2017). The polyphased tectonic evolution of the Anegada Passage in the northern Lesser Antilles subduction zone. *Tectonics*, *36*, 945–961. https://doi.org/10.1002/2017TC004511

Lebrun, J.-F., Lallemand, S., Marcaillou, B., Klingelhoefer, F., Agranier, A., Arcay, D., et al. (2017). *Crustal structure of Northern Grenada Basin call into question the origin of arc migration in the Lesser Antilles: Preliminary results from GARANTI Cruise*. New Orleans: American Geophysical Union Fall Meetting.

Leever, A. K., Gabrielsen, R. H., Sokoutis, D., & Willingshofer, E. (2011). The effect of convergence angle on the kinematic evolution of strain partitioning in transpressional brittle wedges: Insight from analog modeling and high-resolution digital image analysis. *Tectonics*, *30*, TC2013. https://doi.org/10.1029/2010TC002823

Legendre, L., Philippon, M., Münch, P., Leticée, J. L., Noury, M., Maincent, G., et al. (2018). Trench bending initiation: Upper plate strain pattern and volcanism. Insights from the Lesser Antilles arc, St. Barthelemy Island, French West Indies. *Tectonics*, *37*, 2777–2797. https://doi.org/10.1029/2017TC004921

López, A. M., Stein, S., Dixon, T., Sella, G., Calais, E., Jansma, P., et al. (2006). Is there a northern Lesser Antilles forearc block? *Geophysical Research Letters*, *33*, L07313. https://doi.org/10.1029/2005GL025293

Manaker, D. M., Calais, E., Freed, A. M., Ali, S. T., Przybylski, P., Mattioli, G., et al. (2008). Interseismic plate coupling and strain partitioning in the Northeastern Caribbean. *Geophysical Journal International*, *174*(3), 889–903. https://doi.org/10.1111/j.1365-246X.2008.03819.x

Mann (2007). In W. D. Cunningham, & P. Mann (Eds.), *Global catalogue, classification and tectonic origins of restraining- and releasing bends on active and ancient strike-slip fault systems*, *Geological Society, London,* Special Publications, (Vol. 290, pp. 13–142). https://doi.org/10.1144/SP290.2

Mann, P., & Burke, K. (1984). Neotectonics of the Caribbean. *Reviews of Geophysics*, *22*(4), 309–362. https://doi.org/10.1029/RG022i004p00309

Mann, P., Grindlay, N. R., & Abrams, L. J. (2005). Neotectonics of southern Puerto Rico and its offshore margin. *Geological Society of America Special Papers*, *385*, 173–214. https://doi.org/10.1130/0-8137-2385-X.173

Marcaillou, B., & Klingelhoefer, F. (2013). ANTITHESIS-1-Leg1 Cruise, RV L'Atalante. Cruise *Report*. https://doi.org/10.17600/13010070

Marcaillou, B., and Klingelhoefer, F. 2016. ANTITHESIS-3 Cruise, RV Pourquoi Pas? *Cruise Report*. https://doi.org/10.17600/16001700

Martinez, A., Malavielle, J., Lallemand, S., & Collot, J. Y. (2002). Partition de la déformation dans un prisme d'accrétion sédimentaire en convergence oblique: Approche expérimentale. *Bulletin de la Societe Geologique de France*, *173*(1), 17–24. https://doi.org/10.2113/173.1.17

McCaffrey, R. (1991). Slip vectors and stretching of the Sumatran fore arc. *Geology*, *19*(9), 881. https://doi.org/10.1130/0091-7613(1991)019<0881:SVASOT>2.3.CO;2

McCaffrey, R. (1992). Oblique plate convergence, slip vectors, and forearc deformation. *Journal of Geophysical Research*, *97*(B6), 8905. https://doi.org/10.1029/92JB00483

Philippon, M., & Corti, G. (2016). Obliquity along plate boundaries. *Tectonophysics*, *693*, 171–182. https://doi.org/10.1016/j.tecto.2016.05.033

Pindell, J. L., & Kennan, L. (2009). Tectonic evolution of the Gulf of Mexico, Caribbean and northern South America in the mantle reference frame: An update. *Geological Society, London, Special Publications*, *328*(1), 1.1–1.55. https://doi.org/10.1144/SP328.1

Quebral, R. D., Pubellier, M., & Rangin, C. (1996). The onset of movement on the Philippine Fault in eastern Mindanao: A transition from a collision to a strike-slip environment. *Tectonics*, *15*(4), 713–726. https://doi.org/10.1029/95TC00480

Ranero, C. R., & von Huene, R. (2000). Subduction erosion along the Middle America convergent margin. *Nature*, *404*(6779), 748–752. https://doi.org/10.1038/35008046

Sykes, L. R., Mccann, W. R., & Kafka, A. L. (1982). Motion of Caribbean plate during last 7 millions years and implications for earlier Cenozoic movements. *Journal of Geophysical Research*, *87*(B13), 10656–10676. https://doi.org/10.1029/JB087iB13p10656

Symithe, S., Calais, E., De Chabalier, J. B., Robertson, R., & Higgins, M. (2015). Current block motions and strain accumulation on active faults in the Caribbean. *Journal of Geophysical Research: Solid Earth*, *120*, 3748–3774. https://doi.org/10.1002/2014JB011779

ten Brink, U., Danforth, W., Polloni, C., Andrews, B., Llanes, P., Smith, S., et al. (2004). New seafloor map of the Puerto Rico trench helps assess earthquake and tsunami hazards. *Eos, Transactions American Geophysical Union*, *85*(37), 349–360. https://doi.org/10.1029/2004EO370001

ten Brink, U., & Lin, J. (2004). Stress interaction between subduction earthquakes and forearc strike-slip faults: Modeling and application to the northern Caribbean plate boundary. *Journal of Geophysical Research*, *109*, B12310. https://doi.org/10.1029/2004JB003031

Tsuji, T., Ashi, J., & Ikeda, Y. (2014). Strike-slip motion of a mega-splay fault system in the Nankai oblique subduction zone. *Earth, Planets and Space*, *66*, 1–14.

Turner, H. L., Jansma, P. E., Mattioli, G. S., Matson, S., and Rodríguez Cesaní, H. M. 2008. Yes, there is a Northern Lesser Antilles forearc sliver: Results from a decade of GPS observations. In. AGU Fall Meeting San Francisco.

Zelt, C. A., & Smith, R. B. (1992). Seismic traveltime inversion for 2 D crustal velocity structure. *Geophysical Journal International*, *108*(1), 16–34. https://doi.org/10.1111/j.1365-246X.1992.tb00836.x